IEEE Access
Multidisciplinary | Rapid Review | Open Access Journal

Received March 3, 2020, accepted March 16, 2020, date of publication March 18, 2020, date of current version March 31, 2020.

Digital Object Identifier 10.1109/ACCESS.2020.2981840

Robust Integral State Feedback Using Coefficient Diagram in Magnetic Levitation System

ISWANTO ISWANTO[1] AND ALFIAN MA'ARIF[2]
[1]Universitas Muhammadiyah Yogyakarta, Yogyakarta 55183, Indonesia
[2]Department of Electrical Engineering, Universitas Ahmad Dahlan, Yogyakarta 55166, Indonesia

Corresponding author: Alfian Ma'arif (alfianmaarif@ee.uad.ac.id)

This work was supported in part by the Universitas Muhammadiyah Yogyakarta Grant, and in part by the Universitas Ahmad Dahlan Grant.

ABSTRACT Magnetic Levitation System or Maglev system is a modern and future technology that has many advantages and applications. Its characteristic is highly nonlinear, fast dynamics, and unstable, so it is challenging to make a suitable controller. The model of the Maglev system is in nonlinear state-space representation, and then feedback linearization is implemented to obtain the linear model system. Then, the integral state feedback control that tuned by the coefficient diagram method is implemented. The robustness of the controller is determined using the coefficient diagram method. The result of the standard coefficient diagram parameter will be compared with the robustness parameter. The open-loop test simulation showed that the maglev system has a nonlinear characteristic. Among all of the uncertainties, the uncertainty of resistance provides the highest nonlinearity, even by the small value of uncertainty. The examination of the mass, inductance, and resistance uncertainties showed that the robustness parameter is able to handle them and to provide a robust controller.

INDEX TERMS State feedback, robust control, coefficient diagram method, magnetic levitation, integral control.

I. INTRODUCTION

The Maglev (the short of Magnetic Levitation) System is a modern and future technology that levitates an object using electromagnetic force. The simplest maglev system is shown in Fig. 1. It consists of an object from an iron or steel ball, the inductor to generate electromagnet force, a driver to generate a voltage, a controller (Microprocessor or something else), and a sensor to measure the object's height from the inductor. It has a contactless and frictionless characteristic. Thus, it can give high efficiency (almost one hundred percent) [1].

The application of maglev is the maglev train [2] [3], bearing [4], wind turbine [5], suspension [6], [7], and vehicles [8]. Maglev can give high efficiency so that a maglev train that can reach 600 km/hour speed, and maglev wind turbine produces power ten times bigger than a standard wind turbine.

In a maglev system, the electromagnetic force from the inductor must greater than or equal with the gravity force of its object weight. It should be generated fast so that the object does not fall down. Therefore, a maglev system has fast dynamic characteristics.

The associate editor coordinating the review of this manuscript and approving it for publication was Hao Luo.

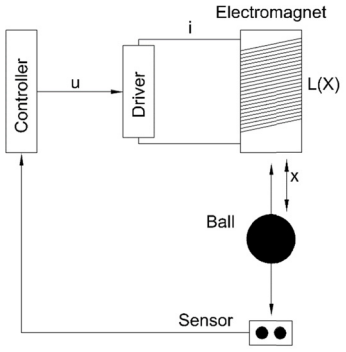

FIGURE 1. The simplest magnetic levitation ball systems.

Another challenge comes from the uncertainty parameter of the inductor when its temperature increases. Besides, it still has some amount of electromagnetic force even though it is not supplied by electrical power. This made a maglev system has uncertainty and highly nonlinear characteristics.

Based on its natural characteristics, a maglev system needs a highly robust controller. It is beneficial to design a suitable controller to control the object's height position, which can accommodate the uncertainty of the maglev system's

parameters and its fast dynamic characteristics. The tuning of parameter controllers also plays an important role in the effectiveness and efficiency of the controller; hence a trial and error method should be avoided. A standard method to tune the controller's parameters is needed to guarantee the high performance of the augmented system.

There are some proposed methods to control the maglev system such as PID controller [9], the fuzzy logic controller [10], [11], LQR [12], Fault-tolerant control and state observer [13], nonlinear power shaping [14], sliding mode control [15], Global Sliding Mode Control [16], Modified Sliding Mode Control [17], feedback linearization [18] and back-stepping [19]. Each of them has its own advantages and disadvantages. A linear control is not suitable for a maglev system, while nonlinear controllers need complex mathematical analysis to match the system model.

Therefore, it is best to combine both nonlinear controllers with linear control to provide a simple controller yet robust and effective to control the maglev system. In the research, the simplest nonlinear control feedback linearization was used to convert the nonlinear model to a linear model. Hence, a linear controller, state feedback control [20], can be implemented. A modification of state feedback control is then proposed by adding integral control to eliminate the steady-state error of the system.

The state feedback controller is a controller in the modern control system that supports multiple inputs and multiple outputs (MIMO) and uses state-space model representation. Based on the previous work [21], a process to determine the controller's parameters always become a problem. It is very important to choose the correct parameter value because it will affect the augmented system performance. Because of that, the coefficient diagram method (CDM) [22], [23] was used to solve the problem. The CDM, which was proposed by Manabe, could avoid the trial and error [24]. It has a standard parameter, and the system performance can be chosen based on it. The standard parameter of CDM is enough to give the best performance from the side of transient-response and steady-state error specifications, but not for the robustness [25].

In the research, uncertainty and disturbance will be used to evaluate the robustness of the proposed controller. The controller is based on a combination of nonlinear and linear control. The nonlinear control used in the proposed controllers is feedback linearization, while the linear control used is state feedback with integral control. Both types of CDM parameters (robust and standard parameter) are used for tuning the controller. The achieved simulation results will then be compared and analyzed.

The paper will be arranged as follows. Section one is the introduction. Section two will discuss the proposed method. Section three will discuss the methodology of the research, which consists of Maglev system modeling, feedback linearization method, integral control with state feedback, Coefficient Diagram Method, and Ackermann's Formula. Section four will provide a result and discussions. The last section will consist of conclusions and future work of the research.

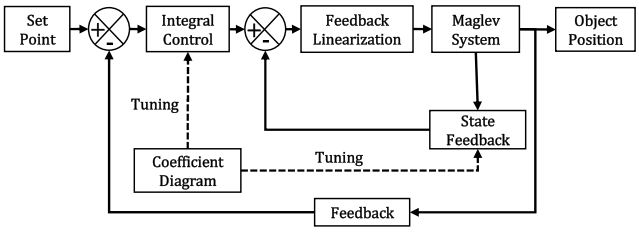

FIGURE 2. The proposed controller system.

II. PROPOSED METHOD

The proposed method in the research is shown in Fig. 2. The Maglev system block is the nonlinear model. The set point is used to give the object reference position, and the proposed method must follow it. Comparing the set point with the feedback will be obtained the difference value or the error value that becomes an input for integral control.

The input of the state feedback block is all of the states, while the feedback only sends one state, the position. The proposed controller consists of the nonlinear control signal from feedback linearization and the linear control signal from state feedback with integral control. The parameter gains of state feedback and integral control will be tuned by using a coefficient diagram with the robustness criteria. The output system is the object position.

III. MODEL OF MAGLEV SYSTEM

There are some methods to determine the model of the maglev system. It can use Newton or Lagrange equations. Generally, it can be generated from a mechanical and electrical analytical point of view. The maglev system model is a nonlinear system. The diagram of the simplest maglev system is shown in Fig. 3.

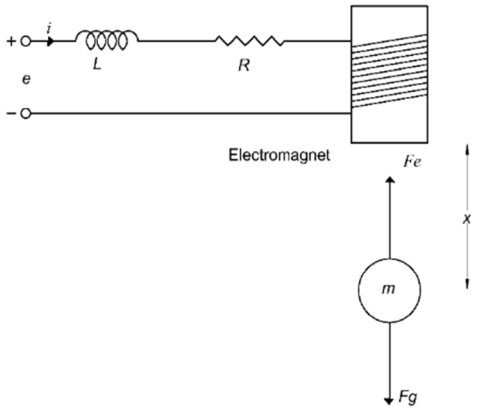

FIGURE 3. The simplest maglev system.

Based on Fig. 3, The inductor produces electromagnetic force, and the object mass produces the gravity force. To levitate the object, the electromagnetic force and the gravity force needs to be equal. If the electromagnetic force is larger

than the gravity force, the object will hit the inductor. Vice versa, if the gravity force is larger than the electromagnetic force, the object will fall.

Based on the mechanical approach using the Newton second law, the dynamic equation of the maglev system in Fig. 3 is,

$$m\frac{d^2x}{dt^2} = mg - k\left(\frac{i}{x}\right)^2 \tag{1}$$

where m is mass of the object, g is the gravity constant, k is the electromagnetic constant, i is current, x is the object position.

Meanwhile, based on the electrical analysis using Kirchhoff's voltage law, the equation is

$$\frac{di}{dt} = -\frac{R}{L}i - \frac{2k}{L}\frac{i}{x^2}\frac{dx}{dt} + \frac{1}{L}e \tag{2}$$

where R is the resistance, L is the inductance, e is the supply voltage.

The state variables must be determined to get a nonlinear state-space model. It could be written as $x_1 = x$ (position), $x_2 = \dot{x}$ (velocity), $x_3 = i$ (current), $u = e$ (applied voltage). Thus, the input model for the maglev system is

$$\begin{bmatrix}\dot{x}_1\\ \dot{x}_2\\ \dot{x}_3\end{bmatrix} = \begin{bmatrix} x_2 \\ -\dfrac{kx_3^2}{mx_1^2} + g \\ -\dfrac{R}{L}x_3 + \dfrac{2k}{L}\left(\dfrac{x_2x_3}{x_1^2}\right)\end{bmatrix} + \begin{bmatrix}0\\0\\\dfrac{1}{L}\end{bmatrix}u. \tag{3}$$

The output model is the position, and it could be written as

$$y = x_1. \tag{4}$$

Based on the input model, it can be known that the maglev system has a nonlinear part, which is shown by the quadratic part of the equation. The nonlinear method was used to eliminate the quadratic part. It was because that the suitable controller to handle nonlinear systems is the nonlinear method. Because of that, the feedback linearization was used.

IV. FEEDBACK LINEARIZATION

The applied feedback linearization in the research is based on Slotine and Li [26] and Khalil [27]. It is used to get the linear model. The idea of Feedback Linearization is to cancel the nonlinearity using a control signal that contains a similar nonlinear part. Thus the model will become an equivalent linear model.

As to implement feedback linearization, the new variables are stated as,

$$z_1 = x_1, \tag{5}$$
$$z_2 = x_2, \tag{6}$$
$$z_3 = g - \frac{kx_3^2}{mx_1^2}. \tag{7}$$

Thus, the new differential equations are,

$$\dot{z}_1 = z_2, \tag{8}$$
$$\dot{z}_2 = z_3, \tag{9}$$
$$\dot{z}_3 = -\frac{2k}{m}\left(\frac{x_3\dot{x}_3}{x_1^2}\right) + \frac{2k}{m}\left(\frac{x_3^2\dot{x}_1}{x_1^3}\right), \tag{10}$$
$$\dot{z}_3 = \alpha(x) + \beta(x)u, \tag{11}$$

where

$$\alpha(x) = -\frac{4k^2x_2x_3^2}{mL_ix_1^4} + \frac{2kRx_3^2}{mL_ix_1^2} + \frac{2kx_3^2x_2}{mx_1^2}, \tag{12}$$
$$\beta(x) = -\frac{2kx_3u}{mx_1^2L_i}. \tag{13}$$

The new state equations are,

$$\dot{z}_1 = z_2, \tag{14}$$
$$\dot{z}_2 = z_3, \tag{15}$$
$$\dot{z}_3 = \alpha(x) + \beta(x)u, \tag{16}$$

The nonlinearity part can be canceled by using the control input u as

$$u = \frac{1}{\beta(x)}(v - a(x)), \quad \beta(x) \neq 0, \tag{17}$$

where v is the new input signal from other controllers. Therefore, the linear state equations become,

$$\dot{z} = \mathbf{A}z + \mathbf{B}u \tag{18}$$
$$y = \mathbf{C}z \tag{19}$$

where

$$\mathbf{A} = \begin{bmatrix}0&1&0\\0&0&1\\0&0&0\end{bmatrix} \quad \mathbf{B} = \begin{bmatrix}0\\0\\1\end{bmatrix} \quad \mathbf{C} = \begin{bmatrix}1&0&0\end{bmatrix} \tag{20}$$

The system is categorized as a 3rd order of the integrator system, which can be written in transfer function representation as

$$\frac{1}{s^3} \tag{21}$$

Hence, the system (21) cannot be controlled by a PID controller as the system has a higher order than a second-order system [28].

V. INTEGRAL STATE FEEDBACK CONTROL

The state feedback is a controller in the modern control system that uses state-space representation. The block diagram of the proposed controller is shown in Fig. 4. The proposed controller consists of state feedback and integral control. The integral control could be known as feed-forward or r-scale technique (another servo state feedback). It is used to eliminate the steady-state error. Meanwhile, state feedback is used to make the system have a good response performance, such as fast rise time, quick settling time, a minimum overshoot without undershooting response. The FL block is the Feedback Linearization (FL), and the MLS block is the Magnetic Levitation System (MLS).

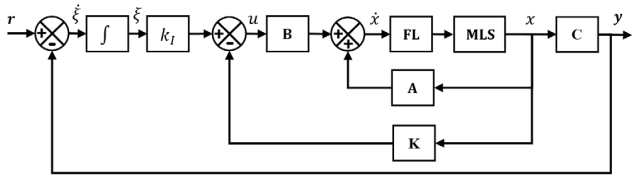

FIGURE 4. Integral state feedback.

Based on Fig. 4, the equations for the system are

$$\dot{x} = \mathbf{A}x + \mathbf{B}u \tag{22}$$
$$y = \mathbf{C}x \tag{23}$$
$$u = -\mathbf{K}x + k_I\xi \tag{24}$$
$$\dot{\xi} = r - y, \tag{25}$$
$$\dot{\xi} = r - \mathbf{C}x, \tag{26}$$

where x is state vector of the plant (n-vector), u is control signal (scalar), y is the output (scalar), r is the reference input signal (step function, scalar), $\mathbf{A}$ is $n \times n$ constant matrix, $\mathbf{B}$ is $n \times 1$ constant matrix, $\mathbf{C}$ is $1 \times n$ constant matrix, k_I is the integral gain, $\mathbf{K}$ is the state feedback gain, ξ is the output the integrator.

Assume the reference signal is step unit,

$$\begin{bmatrix} \dot{x} \\ \dot{\xi} \end{bmatrix} = \begin{bmatrix} \mathbf{A} & 0 \\ -\mathbf{C} & 0 \end{bmatrix} \begin{bmatrix} x \\ \xi \end{bmatrix} + \begin{bmatrix} \mathbf{B} \\ 0 \end{bmatrix} u + \begin{bmatrix} 1 \\ 0 \end{bmatrix} r, \tag{27}$$

For $t > 0$, the state equation is

$$\dot{e} = \widehat{\mathbf{A}}e + \widehat{\mathbf{B}}u_e, \tag{28}$$

where

$$e = \begin{bmatrix} x \\ \xi \end{bmatrix} \quad \widehat{\mathbf{A}} = \begin{bmatrix} \mathbf{A} & 0 \\ -\mathbf{C} & 0 \end{bmatrix} \widehat{\mathbf{B}} = \begin{bmatrix} \mathbf{B} \\ 0 \end{bmatrix} \tag{29}$$

and the overall control signal is

$$u_e = -\widehat{\mathbf{K}}e \tag{30}$$

where

$$\begin{aligned} \widehat{\mathbf{K}} &= \begin{bmatrix} \mathbf{K} & | & -k_I \end{bmatrix} \\ &= \begin{bmatrix} k_1 & k_2 & k_3 & | & -k_I \end{bmatrix} \end{aligned} \tag{31}$$

The state error equation is

$$\dot{e} = (\widehat{\mathbf{A}} - \widehat{\mathbf{B}}\widehat{\mathbf{K}})e \tag{32}$$

The system must be examined first to implement the proposed controller. It is to investigate the system, whether it fulfills the controllability matrix criterion and states controllability or not. The controllability matrix is written as

$$\mathbf{M} = \begin{bmatrix} \mathbf{B} & \mathbf{AB} & \mathbf{A}^2\mathbf{B} \end{bmatrix} \tag{33}$$

and the state controllable matrix is

$$\mathbf{P} = \begin{bmatrix} \mathbf{A} & \mathbf{B} \\ -\mathbf{C} & 0 \end{bmatrix} \tag{34}$$

The rank of the controllability matrix and state controllable matrix will determine the possible arbitrary pole placement. The rank value of the state controllable matrix must be rank > 0 in order to be able to implement the integral state feedback controller.

VI. COEFFICIENT DIAGRAM METHOD

The CDM is proposed by Manabe [29]. It uses a polynomial approach to design a controller. It belongs to the third method in control system design after the classical control system and a modern control system. It is similar to the pole placement method [30] but has standardized parameters.

In pole placement, the pole location can be determined anywhere in s-plane. If the pole is too far from the imaginary axis, the control signal will be too big and unrealistic for real implementation. In CDM, target pole locations are determined based on the specific performance specifications that we want to achieve, for example, settling time less than 5 seconds and no overshoot in response. The desired pole locations are described by the closed-loop polynomial. Hence, the CDM will provide better system response and a more realistic control signal.

Parameters of CDM, such as equivalent time constant and stability index are used to build the target polynomial. These parameters have recommended based on specific functions, i.e. standard and robust parameters.

In CDM, there are open-loop polynomial, the target polynomial, and the closed-loop polynomial. The open-loop polynomial ($\mathbf{P_{OL}}(s)$) is the system characteristic before the controller is implemented, it can be obtained as follow,

$$\mathbf{P_{OL}}(s) = |sI - \mathbf{A}| \tag{35}$$
$$= a_n s^n + a_{n-1}s^{n-1} + \ldots + a_1 s + a_0, \tag{36}$$

Meanwhile, the target polynomial ($\mathbf{P_T}(s)$) is the desired characteristic built of CDM parameters and specific performance specifications that we want to achieve. Later, it is equivalent to the closed-loop polynomial $\mathbf{P_{CL}}(s)$. The closed-loop polynomial contains the target pole locations.

$$\mathbf{P_T}(s) = a_0 \left[\left\{ \sum_{i=2}^{n} \left(\prod_{j=1}^{i-1} \frac{1}{\gamma_{i-j}^{j}} \right) (\tau s)^i \right\} + \tau s + 1 \right] \tag{37}$$

$$\mathbf{P_{CL}}(s) = \alpha_n s^n + \alpha_{n-1}s^{n-1} + \ldots + \alpha_1 s + \alpha_0, \tag{38}$$

where τ is the equivalent time constant, γ is the stability index, α_n is the coefficient, and

$$\alpha_0 = \frac{\prod_{j=1}^{n-1} \gamma_{n-j}^{j}}{\tau^n}. \tag{39}$$

Its parameters (stability index and equivalent time constant) affect the system performances. It can determine the robustness (disturbance rejection) and performance specifications (such as fast settling time). For the best response performances, the standard parameter of CDM can be used.

Based on the Manabe criterion [22], the recommended standard parameter of stability index for (37) to obtain the best system response performance is,

$$\gamma_i = \begin{bmatrix} 2.5 & 2 & 2 & \ldots \end{bmatrix}, \tag{40}$$

While the robust stability index parameter for (37) is

$$\gamma_i = \begin{bmatrix} 4 & 4 & 4 & \dots \end{bmatrix}, \tag{41}$$

for i equal to integer numbers, i.e., 1, 2, 3, and etc. Moreover, the stability index value must not be greater than 4, or it will result in an unrealistic value of control signal.

Furthermore, another parameter is the equivalent time constant τ, which affects the settling time. Smaller values of equivalent time constant provide faster settling time as can be shown as follow,

$$\tau = \frac{t_s}{2.5} \sim \frac{t_s}{3}. \tag{42}$$

The chosen τ then is also used to determine the characteristic of target polynomial in (37). This polynomial then is applied for Ackermann Formula to get the controller gains value.

In CDM, there is a specific graph called a coefficient diagram that provides information about the stability and system response in the logarithmic value. The effect of the stability index and the response is shown in Figure 5. Meanwhile, the effect of the equivalent time constant is shown in Figure 6. Based on the Figure, the x-axis is the i-th coefficient, and the y-axis is the coefficient value based on the closed-loop polynomial in (35).

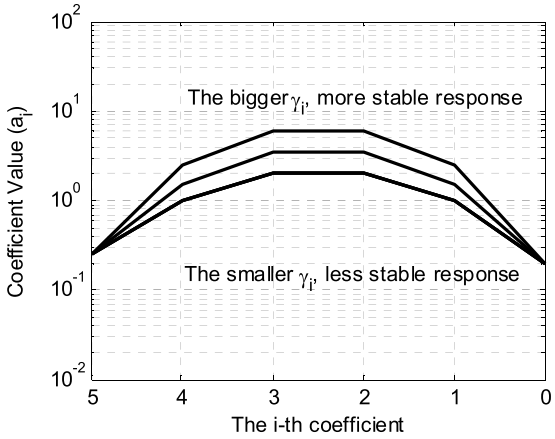

FIGURE 5. The effect of the stability index value.

VII. ACKERMANN'S FORMULA

Consider a system in state-space representation as follows,

$$\dot{\mathbf{x}} = \mathbf{A}\mathbf{x} - \mathbf{B}u \tag{43}$$

and the state feedback control signal is

$$u = -\mathbf{K}\mathbf{x}. \tag{44}$$

Hence, the equation of system (43) with state feedback control (44) becomes

$$\dot{\mathbf{x}} = (\mathbf{A} - \mathbf{B}\mathbf{K})\,\mathbf{x}. \tag{45}$$

Assume that

$$\widetilde{\mathbf{A}} = \mathbf{A} - \mathbf{B}\mathbf{K}, \tag{46}$$

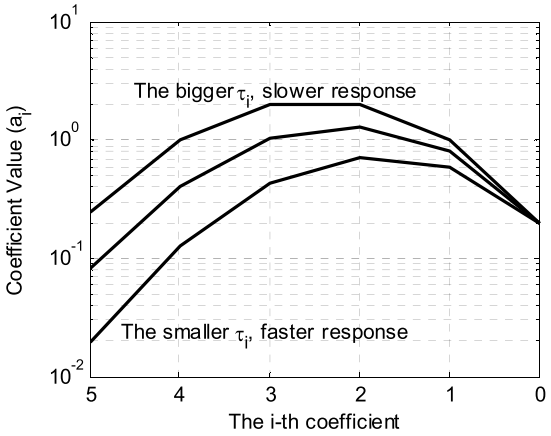

FIGURE 6. The effect of the equivalent time constant.

so that the desired characteristic equation is

$$|s\mathbf{I} - \mathbf{A} + \mathbf{B}\mathbf{K}| = |s\boldsymbol{I} - \widetilde{A}| \tag{47}$$

$$= s^n + \alpha_1 s^{n-1} + \ldots + \alpha_{n-1}s + \alpha_n = 0. \tag{48}$$

Based on the Cayley-Hamilton theorem, $\widetilde{\mathbf{A}}$ satisfied its own characteristic equation as

$$\phi\left(\widetilde{\mathbf{A}}\right) = \widetilde{\mathbf{A}}^n + \alpha_1\widetilde{\mathbf{A}}^{n-1} + \cdots + \alpha_{n-1}\widetilde{\mathbf{A}} + \alpha_n\mathbf{I} = 0 \tag{49}$$

Consider the following identities

$$\mathbf{I} = \mathbf{I} \tag{50}$$

$$\widetilde{\mathbf{A}} = \mathbf{A} - \mathbf{B}\mathbf{K} \tag{51}$$

$$\widetilde{\mathbf{A}}^{\mathbf{2}} = (\mathbf{A} - \mathbf{B}\mathbf{K})^{\mathbf{2}} = \mathbf{A}^{\mathbf{2}} - \mathbf{A}\mathbf{B}\mathbf{K} - \mathbf{B}\mathbf{K}\widetilde{\mathbf{A}} \tag{52}$$

$$\widetilde{\mathbf{A}}^{\mathbf{3}} = (\mathbf{A} - \mathbf{B}\mathbf{K})^{\mathbf{3}} = \mathbf{A}^{\mathbf{3}} - \mathbf{A}^{\mathbf{2}}\mathbf{B}\mathbf{K} - \mathbf{B}\mathbf{K}\widetilde{\mathbf{A}} - \mathbf{B}\mathbf{K}\widetilde{\mathbf{A}}^{\mathbf{2}} \tag{53}$$

Using $n = 3$, the characteristic equation (49) as

$$\alpha_3\mathbf{I} + \alpha_2\widetilde{\mathbf{A}} + \alpha_3\widetilde{\mathbf{A}}^2 + \widetilde{\mathbf{A}}^3$$

$$= \alpha_3\mathbf{I} + \alpha_2\mathbf{A} + \alpha_1\mathbf{A}^2 + \mathbf{A}^3 \tag{54}$$

$$-\alpha_2\mathbf{B}\mathbf{K} - \alpha_1\mathbf{A}\mathbf{B}\mathbf{K} - \alpha_1\mathbf{B}\mathbf{K}\widetilde{\mathbf{A}}$$

$$-\mathbf{A}^{\mathbf{2}}\mathbf{B}\mathbf{K} - \mathbf{A}\mathbf{B}\mathbf{K}\widetilde{\mathbf{A}} - \mathbf{B}\mathbf{K}\widetilde{\mathbf{A}}^{\mathbf{2}} \tag{55}$$

Based on (46), the equation is

$$\alpha_3\mathbf{I} + \alpha_2\widetilde{\mathbf{A}} + \alpha_1\widetilde{\mathbf{A}}^{\mathbf{2}} + \widetilde{\mathbf{A}}^{\mathbf{3}} = \phi\left(\widetilde{\mathbf{A}}\right) = 0 \tag{56}$$

Also

$$\alpha_3\mathbf{I} + \alpha_2\mathbf{A} + \alpha_1\mathbf{A}^{\mathbf{2}} + \mathbf{A}^{\mathbf{3}} = \phi\left(\mathbf{A}\right) \neq 0 \tag{57}$$

Substitute (56) and (57) in α_3 obtained

$$\phi\left(\widetilde{\mathbf{A}}\right) = \phi\left(\mathbf{A}\right) - \alpha_2\mathbf{B}\mathbf{K} - \alpha_1\mathbf{A}\mathbf{B}\mathbf{K}$$

$$-\mathbf{B}\mathbf{K}\widetilde{\mathbf{A}}^{\mathbf{2}} - \alpha_1\mathbf{B}\mathbf{K}\widetilde{\mathbf{A}}$$

$$-\mathbf{A}\mathbf{B}\mathbf{K}\widetilde{\mathbf{A}} - \mathbf{A}^{\mathbf{2}}\mathbf{B}\mathbf{K} \tag{58}$$

Since $\phi\left(\widetilde{\mathbf{A}}\right) = 0$ obtained

$$\phi\left(\mathbf{A}\right) = \mathbf{B}\left(\alpha_2\mathbf{K} - \alpha_1\mathbf{K}\widetilde{\mathbf{A}} - \mathbf{K}\widetilde{\mathbf{A}}^{\mathbf{2}}\right)$$

$$+\mathbf{A}\mathbf{B}\left(\alpha_1\mathbf{K} - \mathbf{K}\widetilde{\mathbf{A}}\right) + \mathbf{A}^{\mathbf{2}}\mathbf{B}\mathbf{K} \tag{59}$$

$$= [\,\mathbf{B} \mid \mathbf{AB} \mid \mathbf{A^2B}] \times \begin{bmatrix} \alpha_2\mathbf{K} - \alpha_1\mathbf{K}\widetilde{\mathbf{A}} - \mathbf{K}\widetilde{\mathbf{A}}^{\mathbf{2}} \\ \alpha_1\mathbf{K} - \mathbf{K}\widetilde{\mathbf{A}} \\ \mathbf{K} \end{bmatrix} \quad (60)$$

Multiplying both sides of (60) by the inverse of the controllability matrix, obtained

$$[\,\mathbf{B} \mid \mathbf{AB} \mid \mathbf{A^2B}]^{-1}\phi(\mathbf{A}) = \begin{bmatrix} \alpha_2\mathbf{K} - \alpha_1\mathbf{K}\widetilde{\mathbf{A}} - \mathbf{K}\widetilde{\mathbf{A}}^{\mathbf{2}} \\ \alpha_1\mathbf{K} - \mathbf{K}\widetilde{\mathbf{A}} \\ \mathbf{K} \end{bmatrix} \quad (61)$$

Multiplying both sides of (58) by $\begin{bmatrix} 0 & 0 & 1 \end{bmatrix}$, obtained

$$\begin{bmatrix} 0 & 0 & 1 \end{bmatrix}\begin{bmatrix} \mathbf{B} \mid \mathbf{AB} \mid \mathbf{A^2B} \end{bmatrix}^{-1}\phi(\mathbf{A}) = \begin{bmatrix} 0 & 0 & 1 \end{bmatrix}\begin{bmatrix} \alpha_2\mathbf{K} + \alpha_1\mathbf{K}\widetilde{\mathbf{A}} + \mathbf{K}\widetilde{\mathbf{A}}^{2} \\ \alpha_1\mathbf{K} + \mathbf{K}\widetilde{\mathbf{A}} \\ \mathbf{K} \end{bmatrix} \quad (62)$$

Which can be written as

$$\mathbf{K} = \begin{bmatrix} 0 & 0 & 1 \end{bmatrix} \begin{bmatrix} \mathbf{B} \mid \mathbf{AB} \mid \mathbf{A^2B} \end{bmatrix}^{-1}\phi(\mathbf{A}). \quad (63)$$

For an arbitrary positive integer n, the state feedback gain is,

$$\mathbf{K} = \begin{bmatrix} 0 & 0 & \cdots & 0 & 1 \end{bmatrix} \begin{bmatrix} \mathbf{B} \mid \mathbf{AB} \mid \cdots \mid \mathbf{B}^{n-1} & \mathbf{B} \end{bmatrix}^{-1}\phi(\mathbf{A}) \quad (64)$$

where

$$\phi(\mathbf{A}) = \mathbf{A}^n + \alpha_1\mathbf{A}^{n-1} + \cdots + \alpha_{n-1}\mathbf{A} + a_n\mathbf{I}. \quad (65)$$

where, α_1 is the coefficient closed-loop polynomial. In MATLAB, the function of Ackermann formula can be applied by using the *acker* command.

VIII. RESULT AND DISCUSSION

There are six examinations that will be simulated. The first examination is coefficient diagram method examination. The next examination is the open-loop stimulation of the maglev system. The next examination is conducted to analyze the proposed controller under the uncertainty of mass, the uncertainty of inductance, the uncertainty of resistance, and disturbance.

The parameters of the Maglev system are as follows. The mass is $0.36kg$, the inductance is $0.12H$, the resistance is 9Ω, the inductor constant is $0.00013Nm^2/A\hat{}2$, the equilibrium position is $0.01m$, and the equilibrium current is $3.2A$. The maximum height of an object is 0.02 meters from the inductor. If the height exceeds the maximum limit, then the examination is considered to fail.

Based on the (34), the rank of the system in (28) is 3, which is rank > 1. Thus, the system completely states controllable. Therefore, the state feedback with integral control is applicable to the system.

TABLE 1. Integral state feedback gains parameter.

Stability Index (γ_i)	Target Closed Loop Polynomial ($\mathbf{P_T}$) and ($\mathbf{P_{CL}}$)	Integral State Feedback Gains $K_e = [K \mid k_I]$
[2.5 2 2]	$s^4 + 20s^3 + 200s^2 + 1000s + 2000$	[1000 200 20 2000]
[4 4 4]	$s^4 + 128s^3 + 4096s^2 + 32768s + 65536$	[32768 4096 128 65536]

A. COEFFICIENT DIAGRAM METHOD EXAMINATION

Based on the CDM, using the standard stability index and the robustness stability index, target closed-loop polynomial in (38), also using the Ackermann's formula in (64), the integral state feedback gains can be obtained. The result of the target closed-loop polynomial and integral state feedback gains is shown in Table 1. The coefficient diagram of the target closed-loop polynomial is shown in Fig. 7.

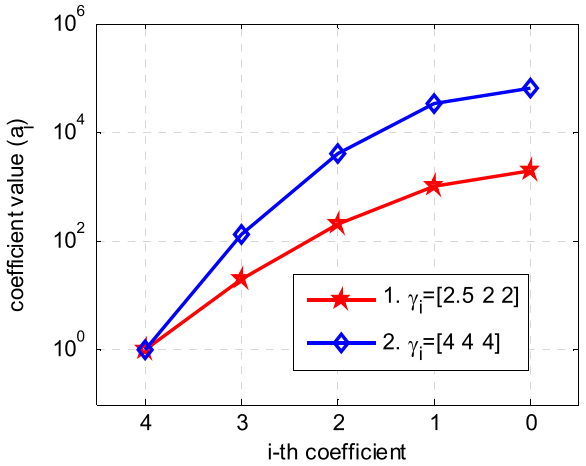

FIGURE 7. Coefficient diagram method.

Fig. 7 is the relation between the stability index to the coefficient value of the closed-loop polynomial. The bigger the stability index, then the coefficients of the closed-loop polynomial are also bigger. Bigger coefficients mean bigger pole values. Bigger poles mean the pole locations are located farther than the imaginary axis, or closer to the infinity value. Meanwhile, it is known that pole locations that provide more stability are the ones located farther from the imaginary axis on the half-left plane. Hence, the bigger value of stability index improves the system's stability better.

The robustness of the system also can be inferred from Fig. 7. The convexity curve of the graph line contains information about stability and robustness. The coefficient curve shape sensibility due to plant parameter variation is a measure of system robustness. The larger and the higher the position of the coefficient curve, the system is more robust to disturbance and more immune to the change of parameters. The blue-colored line is higher and has larger curvature based on the

coefficient diagram so that the system will be more robust to disturbance and uncertainties.

B. OPEN LOOP SIMULATION

The first examination is an open-loop simulation. It is used to determine the characteristics and behavior of the maglev system. It can be shown in Fig. 8. The y-axis is time in second, and the x-axis is the position in the meter.

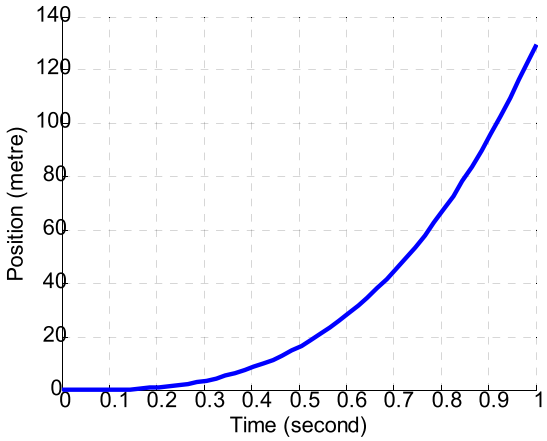

FIGURE 8. Open loop response simulation.

It can be seen in Fig. 8 that the natural characteristics of the system are highly unstable with fast dynamic nonlinear behavior. The system is highly unstable because the response is unbounded while the given input is bounded. Fast dynamic nonlinear can be known from the time needed for the output to get to a certain amplitude; the system can reach 100 meters in position in less than 1 second of simulation time.

C. RESPONSE OF MASS UNCERTAINTY

The examination is done by replacing the ball's mass in a maglev system with varying mass values. The default mass is $0.36kg$, and the examination uses $1kg$ of object mass. The response is shown in Fig. 9. The red line is the response from a standard parameter of CDM, and the blue line is the response from a robust parameter of CDM. The x-axis is the time value, and the y-axis is the object height from the inductor.

Based on Fig. 9, it can be seen that a good system response performance with better disturbance rejection can be achieved from a controller with a stability index parameter as [4 4 4]. Meanwhile, an oscillated response is obtained from the standard parameter of the stability index as [2.5 2 2].

D. RESPONSE OF INDUCTANCE UNCERTAINTY

In this experiment, the test is done by changing the inductance value at specific seconds. The experimental results are shown in Fig. 10, and the changes in the inductance value are set at the third second. The default inductance value is 9H, and the examination uses 9.1H of inductance. Based on the test in Fig. 10, the stability index with a value of [4 4 4] is more robust against changes in the value of resistance. Meanwhile, the

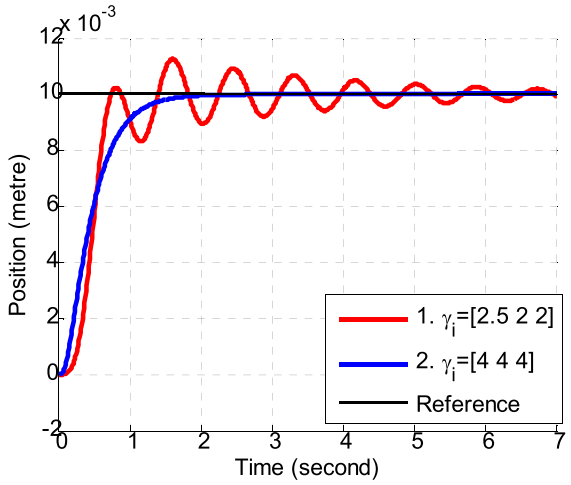

FIGURE 9. The response of mass uncertainty.

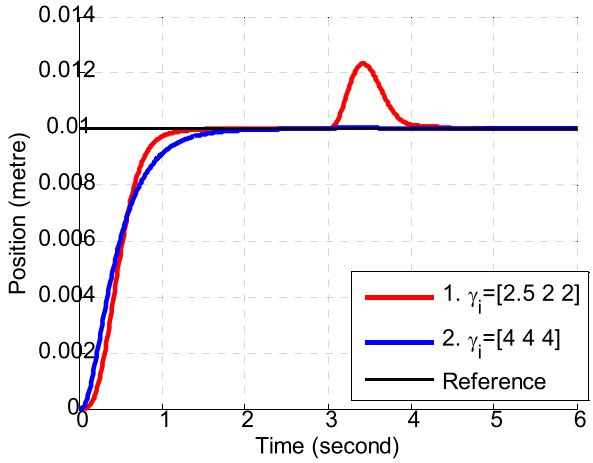

FIGURE 10. The response of inductance uncertainty.

stability index with a value of [2.5 2 2] is highly affected by changes in the resistance value, giving overshoot in response. However, it is able to stabilize the change of the value and to return to its preferred position with a longer time than the use of [4 4 4] parameters. Moreover, these results can still be tolerated because they do not exceed the maglev system height limit of 0.02 meters.

E. RESPONSE OF RESISTANCE UNCERTAINTY

In this experiment, the test is done by changing the resistance value at specific seconds. The experimental results are shown in Fig. 11. and the changes in the resistance value are set at the third second. The default resistance value is 0.12Ω, and the examination uses 0.15Ω of resistance. Based on the test in Fig. 11, the stability index with a value of [4 4 4] is more robust against changes in the value of resistance. It even looks like the augmented system did not get affected at all with the uncertainty. Meanwhile, the stability index with a value of [2.5 2 2] makes the augmented system affected by changes in the resistance value. However, it is still able to return to the preferred position. These results can still be tolerated because

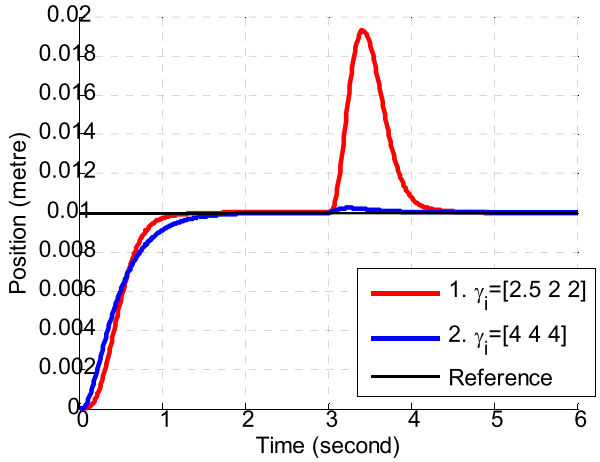

FIGURE 11. The response of resistance uncertainty.

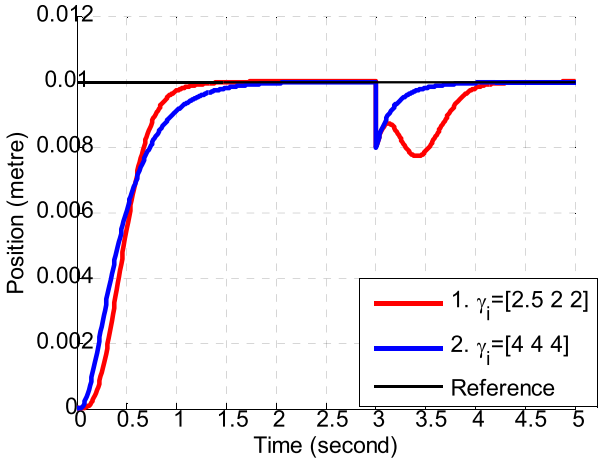

FIGURE 12. The response of disturbance.

they do not exceed the maglev system height limit of 0.02 meters.

F. RESPONSE OF DISTURBANCE

In the test, a disturbance is given to the system in the third second of the simulation time. The test result is shown in Fig. 12. The blue-colored line represents the system response when the robust parameters are implemented to the controller. Meanwhile, the red-colored line shows the system response when a standard parameter is used in the controller. Based on the test result, the implementation of robust parameters to the controller provides a faster and smaller undershoot response in stabilizing the system back to the reference target after the disturbance is given. However, the standard parameter provides a faster rise time before the disturbance is given while the robust parameter makes the system respond a bit slower.

IX. CONCLUSION

Based on the simulation results, it can be concluded that the coefficient diagram method can provide parameter gains that fulfill robustness criteria from disturbance and uncertainties without compromising the object position of the maglev system. Moreover, the standard parameter of CDM is not suitable for a system with high disturbance and uncertainties. The best parameter of stability index for robustness criterion is [4 4 4] which guarantees both zero steady-state error and best disturbance and uncertainties rejection.

ACKNOWLEDGMENT

The authors would like to express gratitude to the editors and blind reviewers for their advice and suggestion to improve the quality of the paper.

REFERENCES

[1] H. S. Han and D. S. Kim, *Magnetic Levitation: Maglev Technology and Applications*. Amsterdam, The Netherlands: Springer, 2016.
[2] J. Xu, Y. Sun, D. Gao, W. Ma, S. Luo, and Q. Qian, "Dynamic modeling and adaptive sliding mode control for a maglev train system based on a magnetic flux observer," *IEEE Access*, vol. 6, pp. 31571–31579, 2018.
[3] Y. Li, D. Zhou, P. Cui, P. Yu, Q. Chen, L. Wang, and J. Li, "Dynamic performance optimization of electromagnetic levitation system considering sensor position," *IEEE Access*, vol. 8, pp. 29446–29455, 2020.
[4] Y. Park, "Design and implementation of an electromagnetic levitation system for active magnetic bearing wheels," *IET Control Theory Appl.*, vol. 8, no. 2, pp. 139–148, Jan. 2014.
[5] Y. Yu, X. Sun, and W. Zhang, "Modeling and decoupling control for rotor system in magnetic levitation wind turbine," *IEEE Access*, vol. 5, pp. 15516–15528, 2017.
[6] A. V. Kireev, N. M. Kozhemyaka, and G. N. Kononov, "Potential development of vehicle traction levitation systems with magnetic suspension," *Int. J. Power Electron. Drive Syst.*, vol. 6, no. 1, pp. 26–31, 2015.
[7] C. Chen, J. Xu, W. Ji, L. Rong, and G. Lin, "Sliding mode robust adaptive control of maglev Vehicle's nonlinear suspension system based on flexible track: Design and experiment," *IEEE Access*, vol. 7, pp. 41874–41884, 2019.
[8] T. Gao, J. Yang, L. Jia, Y. Deng, W. Zhang, and Z. Zhang, "Design of new energy-efficient permanent magnetic maglev vehicle suspension system," *IEEE Access*, vol. 7, pp. 135917–135932, 2019.
[9] Q. Chen, Y. Tan, J. Li, and I. Mareels, "Decentralized PID control design for magnetic levitation systems using extremum seeking," *IEEE Access*, vol. 6, pp. 3059–3067, 2018.
[10] E. A. De Freitas Nunes, A. O. Salazar, E. R. Llanos Villarreal, F. E. C. Souza, L. P. Dos Santos, J. S. B. Lopes, and J. C. C. Luque, "Proposal of a fuzzy controller for radial position in a bearingless induction motor," *IEEE Access*, vol. 7, pp. 114808–114816, 2019.
[11] J. Zhang, X. Wang, and X. Shao, "Design and real-time implementation of Takagi–Sugeno fuzzy controller for magnetic levitation ball system," *IEEE Access*, vol. 8, pp. 38221–38228, 2020.
[12] F. Ni, Q. Zheng, J. Xu, and G. Lin, "Nonlinear control of a magnetic levitation system based on coordinate transformations," *IEEE Access*, vol. 7, pp. 164444–164452, 2019.
[13] M. Zhai, Z. Long, and X. Li, "Fault-tolerant control of magnetic levitation system based on state observer in high speed maglev train," *IEEE Access*, vol. 7, pp. 31624–31633, 2019.
[14] L. Qi, J. Cai, A. Han, J. Wan, C. Mei, and Y. Luo, "A novel nonlinear control technique with its application to magnetic levitated systems," *IEEE Access*, vol. 6, pp. 78659–78665, 2018.
[15] S. Saha, S. M. Amrr, M. U. Nabi, and A. Iqbal, "Reduced order modeling and sliding mode control of active magnetic bearing," *IEEE Access*, vol. 7, pp. 113324–113334, 2019.
[16] R. Uswarman, A. I. Cahyadi, O. Wahyunggoro, R. Uswarman, A. I. Cahyadi, and O. Wahyunggoro, "Design and implementation of a magnetic levitation system controller using global sliding mode control," *J. Mechtron., Elect. Power, Veh. Technol.*, vol. 5, no. 1, p. 17, Jul. 2014.
[17] R. Uswarman, A. I. Cahyadi, and O. Wahyunggoro, "Modified sliding mode control with uncertainties behavior of a magnetic levitation system," in *Proc. Int. Conf. Robot., Biomimetics, Intell. Comput. Syst.*, Nov. 2013, pp. 194–199.

[18] R. Uswarman, A. I. Cahyadi, and O. Wahyunggoro, "Control of a magnetic levitation system using feedback linearization," in *Proc. Int. Conf. Comput., Control, Informat. Its Appl. (ICINA)*, Nov. 2013, pp. 95–98.
[19] A. S. Malik, I. Ahmad, A. U. Rahman, and Y. Islam, "Integral backstepping and synergetic control of magnetic levitation system," *IEEE Access*, vol. 7, pp. 173230–173239, 2019.
[20] K. Ogata, *Modern Control Engineering*. Upper Saddle River, NJ, USA: Prentice-Hall, 2010.
[21] A. Ma'arif, A. I. Cahyadi, and O. Wahyunggoro, "CDM based servo state feedback controller with feedback linearization for magnetic levitation ball system," *Int. J. Adv. Sci., Eng. Inf. Technol.*, vol. 8, no. 3, p. 930, Jun. 2018.
[22] Y. C. Kim and S. Manabe, "Introduction to coefficient diagram method," *IFAC Proc. Volumes*, vol. 34, no. 13, pp. 147–152, Aug. 2001.
[23] H. Ali, G. Magdy, B. Li, G. Shabib, A. A. Elbaset, D. Xu, and Y. Mitani, "A new frequency control strategy in an islanded microgrid using virtual inertia control-based coefficient diagram method," *IEEE Access*, vol. 7, pp. 16979–16990, 2019.
[24] A. Ma'arif, A. I. Cahyadi, O. Wahyunggoro, and Herianto, "Servo state feedback based on coefficient diagram method in magnetic levitation system with feedback linearization," in *Proc. 3rd Int. Conf. Sci. Technol. Comput. (ICST)*, Jul. 2017, pp. 22–27.
[25] S. Manabe, "Coefficient diagram method," *IFAC Proc. Volumes*, vol. 31, no. 21, pp. 211–222, Aug. 1998.
[26] J. J. E. Slotine and W. Li, *Applied Nonlinear Control*. Upper Saddle River, NJ, USA: Prentice-Hall, 1991.
[27] H. K. Khalil, *Nonlinear Systems: Pearson New International Edition*. London, U.K.: Pearson, 2013.
[28] A. Maarif, A. I. Cahyadi, S. Herdjunanto, Y. Yamamoto, and Iswanto, "Tracking control of higher order reference signal using integrators and state feedback," *IAENG Int. J. Comput. Sci.*, vol. 46, no. 2, pp. 208–216, Jun. 2019.
[29] S. Manabe, "Importance of coefficient diagram in polynomial method," in *Proc. 42nd IEEE Int. Conf. Decis. Control*, Dec. 2003, pp. 3489–3494.
[30] J. P. Coelho, T. M. Pinho, and J. Boaventura-Cunha, "Controller system design using the coefficient diagram method," *Arabian J. Sci. Eng.*, vol. 41, no. 9, pp. 3663–3681, Sep. 2016.

ISWANTO ISWANTO was born in Yogyakarta, Indonesia. He received the S.T., M.Eng., and Dr.Eng. degrees from the Department of Electrical Engineering, Universitas Gadjah Mada.

He is currently a Lecturer with the Department of Electrical Engineering, Universitas Muhammadiyah Yogyakarta. His research interests include instrumentation, control systems, robotics, and artificial intelligence.

Dr. Iswanto is the Editor-in-Chief of the *Journal of Robotics and Control* (JRC) and a Reviewer of the *International Journal of Electrical and Computer Engineering* (IJECE).

ALFIAN MA'ARIF was born in Klaten, Central Java, Indonesia, in 1991. He received the S.T. degree from the Department of Electrical Engineering, Universitas Islam Indonesia, in 2014, and the M.Eng. degree from the Department of Electrical Engineering, Universitas Gadjah Mada, in 2017.

From 2017 to 2018, he was a Lecturer with the Department of Electrical Engineering Education, Universitas Negeri Yogyakarta. Since 2018, he has been a Lecturer with the Department of Electrical Engineering, Universitas Ahmad Dahlan. His research interests include robotics, control systems, and computer programming.

Mr. Alfian is a member of IAENG and IAES. He is a Section Editor of *Telecommunication Computing Electronics and Control* in control system field, a Managing Editor of the *Journal of JITEKI* and the *Journal of Robotics and Control* (JRC), and a Reviewer of IEEE Access.